International Journal of Electrical and Computer Engineering (IJECE)
Vol. 16, No. 2, April 2026, pp. 651~662
ISSN: 2088-8708, DOI: 10.11591/ijece.v16i2.pp651-662

Single-stage single-phase grid connected inverter proportional resonant and maximum power point tracking controllers for enhanced photovoltaic system performance

Abdelaziz Kabba, Abdellah Lassioui, Hassan El Fadil
ASE-Laboratory, ENSA, Ibn Tofail University, Kenitra, Morocco

Article Info

Article history:

Received Jul 31, 2024
Revised Jan 3, 2026
Accepted Jan 16, 2026

Keywords:

Lyapunov stability
Maximum power point tracker
Phase locked loop
Photovoltaic
Power factor controller
Proportional resonant controller

ABSTRACT

The paper develops a current control methodology for a single-phase grid-tied DC/AC inverter applied to photovoltaic (PV) energy conversion systems. It incorporates an algorithm for finding the optimal voltage and current points to obtain maximum power point tracking (MPPT), the purpose of which is to ensure better energy extraction. This is followed by a proportional-integral (PI) controller to generate the reference current. In addition, a proportional-resonant (PR) controller is used to infinitely amplify the fundamental frequency signal, which makes it possible to eliminate the steady-state error. The analytical foundations of the PR controller are presented and substantiated through simulation studies implemented in MATLAB/Simulink. The phase-locked loop (PLL) is used for synchronization, enabling accurate phase detection of the grid voltage for effective power injection. An LCL filter is also implemented between the inverter and the grid. The results provided by the dedicated software confirm the effectiveness of the proposed control system.

Corresponding Author:

Abdelaziz Kabba
ASE-Laboratory, ENSA, Ibn Tofail University
44 Lot Alothmania Tr 3 Meknes, 50000, Morocco
Email: kabbaziz.70@gmail.com

1. INTRODUCTION

Renewable energies represent a viable pathway toward lowering pollution levels. In particular, In recent years, photovoltaic (PV) solar energy has undergone substantial growth worldwide, as it is an inexhaustible, environmentally-friendly and silent source [1], [2]. The rapid development of solar power is gradually being implemented in small-scale installations connected to the low-voltage (LV) grid [3], [4] to solar farm installations directly connected to the medium-voltage (MV) grid. Several solutions are available to increase electricity production capacity, including the periodic removal of dust from photovoltaic modules. Study [5] presents the design and development of a robot for cleaning photovoltaic modules.

However, the large-scale integration of PV sources into the grid introduces additional complexities [6] and some challenges that need to be overcome in order to ensure the smooth integration of solar power on power grids [7]. The main problem lies in managing the intermittency of solar power generation, which depends on external factors such as insolation and temperature, influencing the modification of power flows (bidirectional), on the voltage plane, on the protection plane. Grid stability can be affected by high solar irradiation or energy shortages, which can disrupt the frequency and voltage of the power grid. These fluctuations need to be controlled to avoid outages or damage to network equipment, while complying with technical standards [8]. The operating conditions demanded by regulation devices, such as intelligent inverters and energy storage systems (batteries), are necessary to adjust energy production and injection into

the power grid according to needs, while guaranteeing power quality. This observation is prompting researchers to present new research and technological solutions aimed at secure, reliable, and efficient network connectivity.

In the literature, in grid-connected mode with a single phase or more, a PV system can be divided into two subsystems: a power subsystem consisting of PV panels, DC/DC and DC/AC converters followed by an intermediate filter [9] where the DC/AC inverter, is regarded as central component due to its crucial role in grid-connected operation [10] and a maximum power point tracking (MPPT) control subsystem and other converter control blocks used. In general, the first subsystem is controlled to have high power, whatever the weather conditions, and ensure power factor correction (PFC) to reduce current harmonics in converters and optimize active power exchanged between energy source and grid [11]. In [12], numerous control methods are proposed. Indeed, a passive technique is studied in [13], while controllers (PR) and multi resonant control (MRC) have been discussed in [14]. In addition to classical methods, there are control techniques that do not require mathematical models, such as genetic algorithms, fuzzy logic and artificial neural networks. Typically, current control is commonly adopted because it offers excellent dynamic response [15], [16] as well as integrated overcurrent protection. Predictive control relies on an accurate system model and reference current prediction [17]. Hysteresis control, though simple and robust, suffers from variable switching rates, doubled current errors, and limited high-frequency operation [18]. Various MPPT methods have been proposed [19]. In study [20], a recalibrated fractional order proportional-integral-derivative (FOPID) compensator controlling the output voltage error of an interleaved buck–boost converter is applied for MPPT, while [21] utilizes a non-inverting buck–boost converter with GGSMC feedback to track an feed forward neural network-generated voltage reference and extract the PV system's maximum power. A simple and commonly used approach is the perturbation and observation (P&O) method, which involves perturbing the operating voltage of the photovoltaic array, causing the system to oscillate around the optimal power. The magnitude of these oscillations can be minimized by reducing the disturbance step size, enabling the reference voltage V_{dc}^{*} to be accurately determined during periodic operation. Additionally, an H∞ approach was developed in [22] for a two-stage low-voltage topology, ignoring the PV array's nonlinear P(V) characteristic. The same limitation occurs in [23], which proposed a nonlinear predictive proportional-integral (PI) controller. The control of the intermediate DC bus has been widely studied [24]. To prevent start-up stalling and guarantee MPPT, the error signal ε_{dc}=(V_{dc}-V_{dc}^{*}) at the regulator input is inverted compared to the conventional configuration.

2. PROPOSED STUDY

The article proposes a new architecture for connecting the photovoltaic (PV) system to the grid, enabling more stable and efficient integration. It is based on the resonant proportional controller (PR), which plays an essential role in this connection, particularly at the inverter level. It regulates the injected current by following a sinusoidal reference (generally at 50 Hz), something that conventional controllers such as the PI, have difficulty achieving with precision at steady state. Designed to offer high gain at this frequency, it ensures precise following of the sinusoidal waveform while eliminating steady-state error. What's more, it helps reduce harmonics and stabilize the current waveform, improving grid compatibility. Finally, it offers compatibility with real-time operation unlike PI controllers, the PR operates efficiently in the stationary reference frame (αβ), simplifying implementation in single-phase or three-phase inverters without coordinate transformation. The system illustrated in Figure 1 has the advantage of using a single DC/AC stage, without using a transformer for matching as in [25]. Acting as a decoupling energy reservoir, the DC-side capacitor enables energy transfer to the AC circuit.

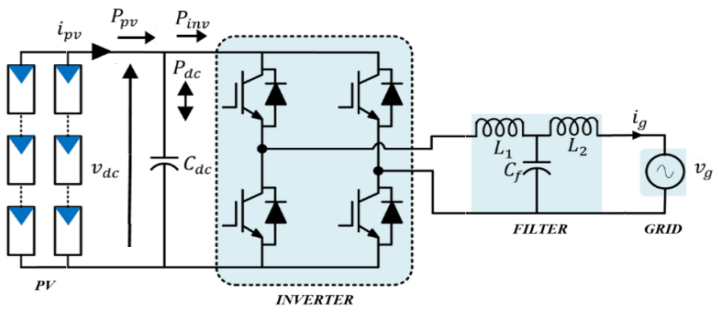

Figure 1. Basic diagram of PV system connected grid

The AC terminal filter of converters (on the grid side) generally has much less stored energy. Consequently, its impact on power transmission can be considered negligible [26]. For stability analysis, the defined Lyapunov function only takes into account the dynamics of the energy stored in the capacitor downstream of the PV, which must be sufficiently large. This approach is adapted by the authors for three-phase PV inverters with a low-value coupling capacitor, since the continuous power does not exhibit oscillations [27]. In addition to system stability, the study also addresses the following objectives: i) to apply an MPPT strategy to extract maximum power from the PV modules, enhancing the energy efficiency of the array; ii) to implement a PI controller for the DC bus voltage considering the P–V curve; and iii) to use a PR controller to inject a sinusoidal current in phase with the grid voltage, with grid synchronization ensured via a phase-locked loop (PLL) tracking the voltage fundamental [18].

The MPPT block, using a P&O algorithm as illustrated in the flowchart in Figure 2, combined with a PI proportional-integral voltage controller, forms the outer loop of the system which determines the grid reference current I_{ref} required to regulate the string PV generator to impose a reference voltage V_{dc}^{*}. As for the internal loop, it is designed to control the currents supplied by the inverter i_{inv} and those injected into the grid i_g [28], and Figure 3 illustrates these main devices required for the control of the proposed system.

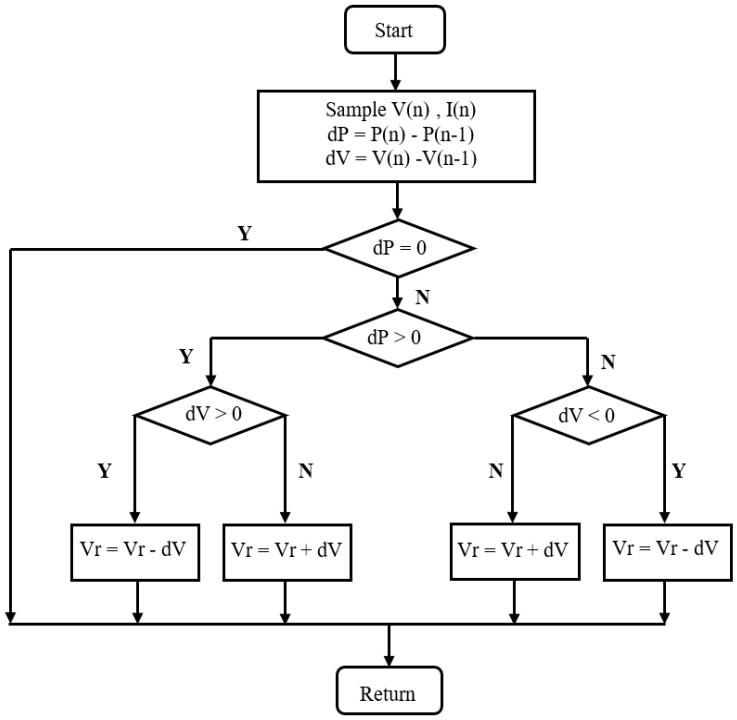

Figure 2. MPPT algorithm flowchart (P&O)

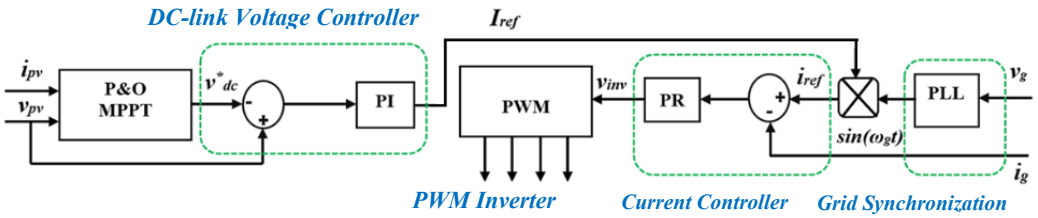

Figure 3. Control structure of the grid-connected single-phase PV inverter

The article is organized as follows: section 3 examines the different powers in order to develop the system's control strategy. Section 4 discusses stability in relation to the fact that the P(V) characteristic is nonlinear and affects its effect on the intermediate circuit voltage. Section 5 aims to validate the analytical demonstration with MATLAB/Simulink simulations. Section 6 concludes the article.

3. CONTROL STRATEGY

3.1. Description of the different power ratings

In Figure 1, the PV system uses an inverter as a bridge to connect to the grid. To simplify the study, we assume that: i) The inverter, the coupling capacitor with PV, and the output filter do not exhibit power losses. And ii) Other terms representing conduction losses can be neglected.

For the power balance in the DC bus, we can write:

$$P_v(t) = P_{dc} + P_g \tag{1}$$

as: $P_{inv} = P_g$. The power in the grid is given by:

$$p_g = v_g(t) i_g(t) = V_g I_g (1 - cos\, 2\,\omega t) \tag{2}$$

Where v_g, i_g are instantaneous grid voltage and grid current respectively; I_g, V_g are root mean square (RMS) of current i_g and v_g respectively; and ω: grid pulsation.

The power injected into the single-phase P_{grid} grid, calculated in (2), is sinusoidal and has twice the frequency of the grid. The operation of the PV generator at the maximum power point (MPP) would be compromised if the pulsed power were not attenuated using an energy storage device. Therefore, bus capacitors are generally used to store this energy, and their instantaneous power $Pc(t)$ is equal to:

$$P_{dc}(t) = C_{dc} V_{dc} \frac{dV_{dc}}{dt} \tag{3}$$

The average power of the electrical network is given by:

$$P_{gav} = V_g I_g \tag{4}$$

3.2. Proposed controller

The DC bus voltage controller is used to regulate the DC voltage to a desired level in order to extract maximum power from the photovoltaic array. The non-linear PV characteristic means that changes in irradiance shift the operating point, modifying the DC power and, consequently, the MPP. As the grid voltage remains constant, the power transferred to the grid is controlled entirely by the inverter's output current.

The mathematical model describing the dynamics of power transfer is given by (5):

$$P_{ref} = V_g I_{gref} = V_{pv} I_{pv} - C_{dc} V_{dc} \frac{dV_{dc}}{dt} \tag{5}$$

Where P^*g, I^*g are reference grid power and current respectively; I^*_{iny} are current of the inverter; V_{pv}, i_{pv} are periodic signals having the average components $\bar{V}_{pv}$, $\bar{I}_{pv}$ and the AC components $\tilde{v}_{pv}$, $\tilde{\imath}_{pv}$; and $T = 1/(2f_{grid})$ are oscillation period. V_{pv}, i_{pv} are defined respectively as:

$$\begin{cases} V_{pv} = \bar{V}_{pv} + \tilde{v}_{pv} \\ I_{pv} = \bar{I}_{pv} + \tilde{\imath}_{pv} \end{cases} \tag{6}$$

The power injected into the Pav grid is controlled according to (7), using a term Ppv and a second term kdP/dV that takes into account the system dynamics of the photovoltaic inverter:

$$P_{gref} = V_g I_{gref} = P_{pv} + k \frac{dP}{dV} \tag{7}$$

And by substituting (8) into (5) we get:

$$C_{dc} V_{dc} \frac{dV_{dc}}{dt} = -k \frac{dP}{dV} \tag{8}$$

According to (8), dP/dV depends on the dynamics of capacitor C_{dc}. The alternating waveform components the power PV $\tilde{p}_{pv}$ and the DC bus voltage $\tilde{v}_{dc}$ are estimated using a quadrature signal generator based on a generalized second-order integrator, functioning as a $\pi/2$ phase shifter (Figure 3, closed-loop transfer function in (9)).

The reference current is calculated from the reference PV power supplied by the controller in Figure 4 and the effective value of the grid voltage. The PLL extracts the phase angle of the grid, which is multiplied by the amplitude of the inverter reference current. The current controller then regulates the current injected into the grid i_g. The current control and voltage control loops are illustrated in Figures 5 and 6.

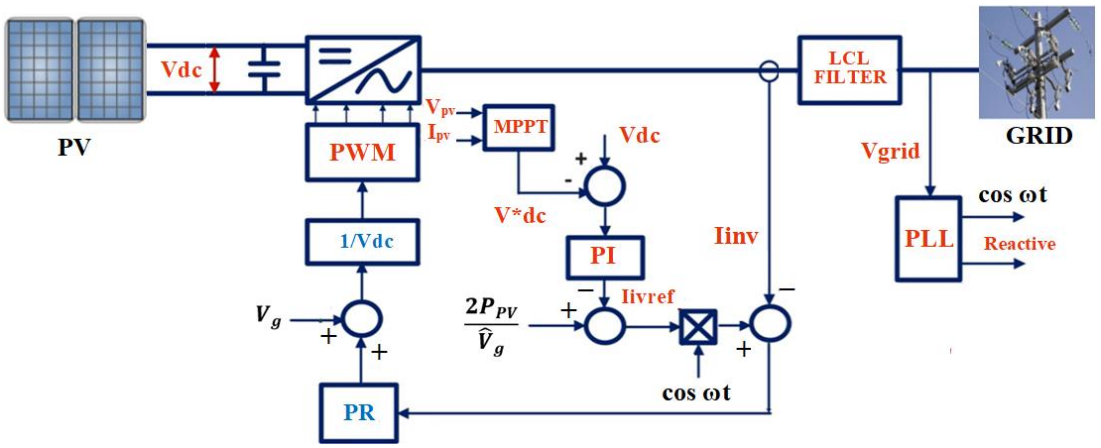

Figure 4. Shows the structure of the controllers controlling the inverter

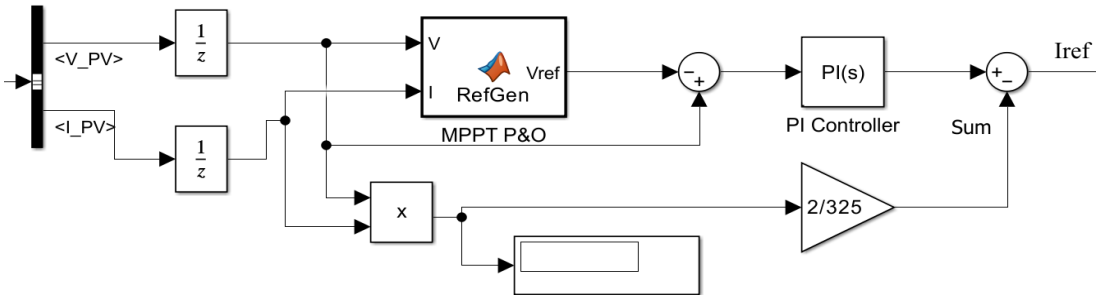

Figure 5. MPPT control and reference current I_{ref} generation loop

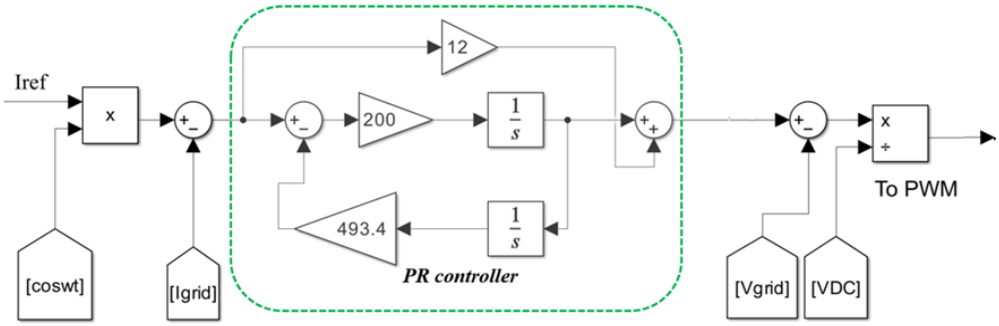

Figure 6. PR based control loop for PWM command generation

3.3. Synchronization with the PLL grid

Connecting the PV source to the electrical network through the DC/AC converter requires synchronization of the voltage produced with that of the network, it is therefore essential to know the phase and frequency of the voltage grid. Most efficient method is the use of a PLL, single-phase PLLs are subject to an additional difficulty than in three-phase, because of the smaller information field (only one phase). To create two orthogonal signals in single-phase, it is necessary to add a "Quadrature" demodulation block in Figure 7.

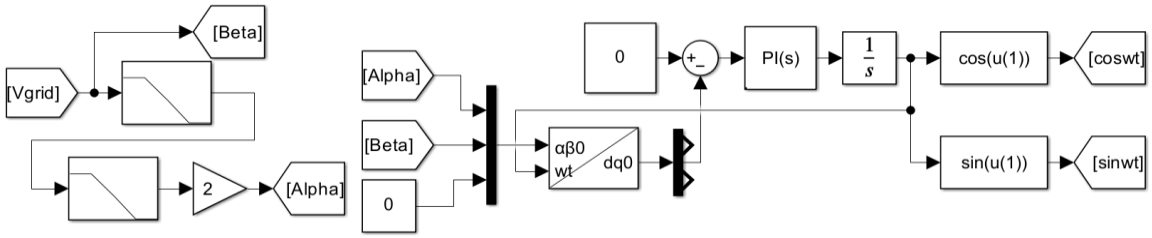

Figure 7. Basic structure of a single-phase PLL

3.4. Transfer function of the resonant controller

In grid-connected photovoltaic systems, the PR current controller is commonly employed to ensure accurate tracking of the sinusoidal current reference injected I^*_g, while guaranteeing zero static error at the fundamental frequency and current quality compliant with grid connection standards. The resonant controller can be described by the following transfer function:

$$T(\omega) = \frac{k_p s^2 + 2k_i s + k_p \omega_n^2}{s^2 + \omega_n^2} \tag{9}$$

The proportional and resonant gains of the PR controller are obtained through a trial-and-error tuning method, first adjusting the proportional gain to ensure system stability and dynamic performance, then the resonant gain to reduce the error in static mode at the synchronism frequency. In particular, we take: the proportional coefficient is: $k_p = 12$, the integral coefficient is: $k_i = 200$ and the pulsation is: $\omega_n = 100\pi$. The amplitude and phase Bode diagrams are represented by Figure 8.

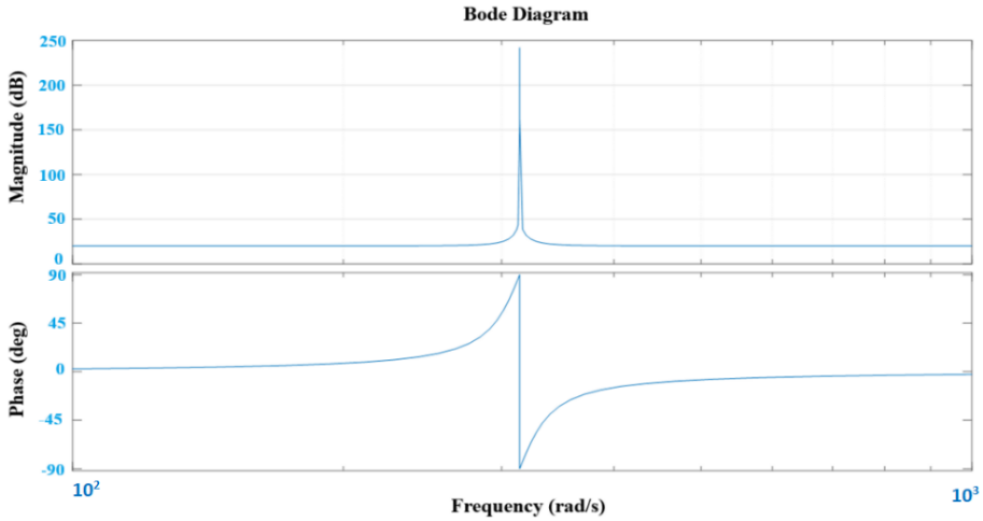

Figure 8. Bode response of the PR controller

4. STABILITY ANALYSIS

Since the system under study exhibits nonlinearity, we define a Lyapunov function $V(x)$ that takes into account the states of the system. Consequently, $V(x)$ will be formed based on the variation in energy stored in the intermediate circuit capacitor, assuming that the effect of the other components is negligible and therefore has no effect on the stability of the system. The candidate function can be written as:

$$V(E_{dc}) = \frac{C_{dc}^2}{4}(V_{dc}^{*2} - V_{dc}^2)^2 \tag{10}$$

Where: $V(E_{dc}) > 0$; E_{dc} is energy stored in C_{dc}.

Figure 4 illustrates the MPPT controller diagram implementing the (P&O) algorithm. This algorithm operates by successive perturbations around the measured voltage V_{dc} in order to generate the optimal reference voltage V_{dc}^{*} in Figure 9(a). The stable maximum power point (PP), defined by the coordinates ($V_{MP} = V_{dc}^{*}$, PM), corresponds to the maximum power achieved at the voltage V_{dc}^{*}. This point is located between the stable and unstable regions of the P(V) characteristic curve traversed during the MPPT tracking process in Figure 9(b). In addition, Figure 9(c) shows the P(V) curves for the PV generator used in the simulation, parameterized by irradiance levels (100 W/m², 500 W/m², and 1000 W/m²). Under identical conditions and following [29], global stability of the system is ensured if $V(E)$ satisfies the following conditions:

$$V(0) = 0 \tag{11}$$

$$V(E_{dc}) > 0 \text{ for all } V(E_{dc}) \neq 0 \tag{12}$$

$$V(E_{dc}) \to \infty \text{ as } |E_{dc}| \to \infty \tag{13}$$

$$\frac{dV(E_{dc})}{dt} < 0 \text{ for all } |E_{dc}| \neq 0 \tag{14}$$

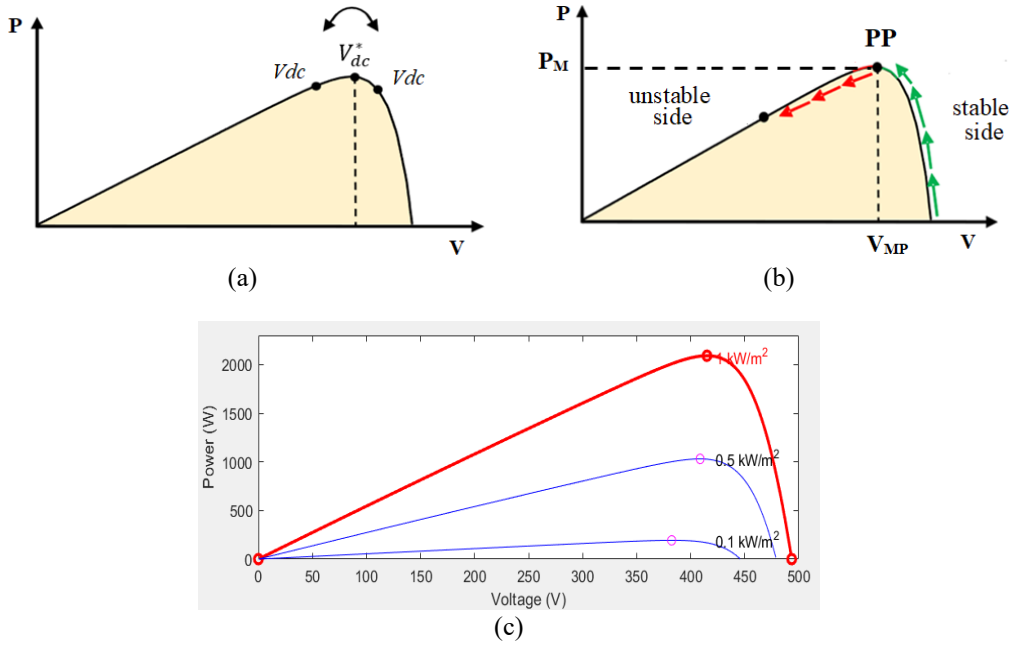

Figure 9. Power curve as a function of voltage P(V), (a) Search for reference voltage V_{dc}^{*}, (b) Stable peak point PP, and (c) Specifications of the curves of the PV source used

It should be noted that the last condition ensures global stability of the system when the stored energy is continuously dissipated ($V(E_{dc}) \times dV(E_{dc})/dt < 0$), which implies a continuous convergence of the system toward its equilibrium point. Hence, the adopted Lyapunov function satisfies the requirements outlined above, and its time derivative $dV(E)/dt$ is given by (11) in the following form:

$$\frac{dV(E_{dc})}{dt} = -C_{dc}^{2} V_{dc} \frac{dV_{dc}}{dt} (V_{dc}^{*} - V_{dc})(V_{dc}^{*} + V_{dc}) \tag{15}$$

Replacing (11) with (5) results in:

$$\frac{dV(E_{dc})}{dt} = -C_{dc}\left(P_{gref} - P_{pv}\right)(V_{dc}^{*} - V_{dc})(V_{dc}^{*} + V_{dc}) \tag{16}$$

In fact, on the basis of (17), as a result, the sign of the derivative of the function $V(E_{dc})$ can be identified, and it evidently depends on the power variation associated with the voltage difference. The

convergence of system stability is evaluated in two cases, as in [29], the system is stable. The reference current is given by (17):

$$I_{invref} = 2\frac{P_{pv}+k(-V_{dc}^{*}+V_{dc})}{\hat{V}_g} \quad (17)$$

5. SIMULATION RESULTS AND DISCUSSION

The system illustrated in Figure 1 is implemented on the MATLAB/Simulink platform, Figure 3 presents the implemented control strategy. In particular, MPPT controller based on the P&O algorithm and using the PI regulator as shown in Figure 5, allows to optimize the photovoltaic energy production. Once the maximum power is extracted from the PV system, this energy is converted by the inverter used. Control is performed through PWM, signals generated efficiently and accurately from a PR controller in Figure 6. Synchronization with the grid frequency is achieved by a PLL based circuit in Figure 7. The type of PV module used is Zytech Engineering Technologie ZT190S, whose P(V) curve for 11 modules in series and for different irradiance values is plotted in Figure 9(c), the parameters of the simulated grid-connected photovoltaic system are listed in Table 1.

Table 1. The performance of system study

PV module	Series connected	Power (kW)	Filter LCL	PWM	GRID
Voc = 44.86 V	11 Modules	2 kW	L_1 = 4 mH	f_P = 10 kHz	Vmax = 325 V
Isc = 5.5 A			C = 6.25 µF		f = 50 Hz
V_{MPP} = 37.73 V	Cdc = 600 µF		L_2 = 4.3 mH		

For the simulation, the P&O algorithm is configured with the following parameters: tracking frequency set at $f_{MPPT} = 1$ Mhz, and the increment voltage ΔV_{MPPT} = 0.5 V, and this with the aim of decreasing oscillations around the MPP and thus reducing steady-state losses. The curves below are for irradiation of 1000 W/m^2 and a temperature of 25 °C (STC conditions). The MPPT algorithm follows the maximum power point (MPP) on the right side of the P(V) curve, as confirmed by the grid voltage in Figure 10 and the DC bus start-up voltage in Figure 11. Once the DC bus capacitor is fully charged, its voltage reaches the voltage (Voc) when it delivers zero current from the PV source. The measured value is approximately 420 V. Thereafter, the DC bus voltage stabilizes, with slight fluctuations around the MPP in steady state, without causing disturbances. Analysis of the DC bus voltage and grid current in Figure 11 shows that the system with the MPPT controller and PI regulator is stable, with the PI regulator effectively reducing fluctuations to compensate for rapid changes in irradiance or load. The analysis of the derivative of the function $V(E_{dc})$, based on (16) and the curve in Figure 12, indicates that after system start-up, $dV(E_{dc})/dt$ remains negative. It gradually approaches zero in steady state, ensuring the overall stability of the system.

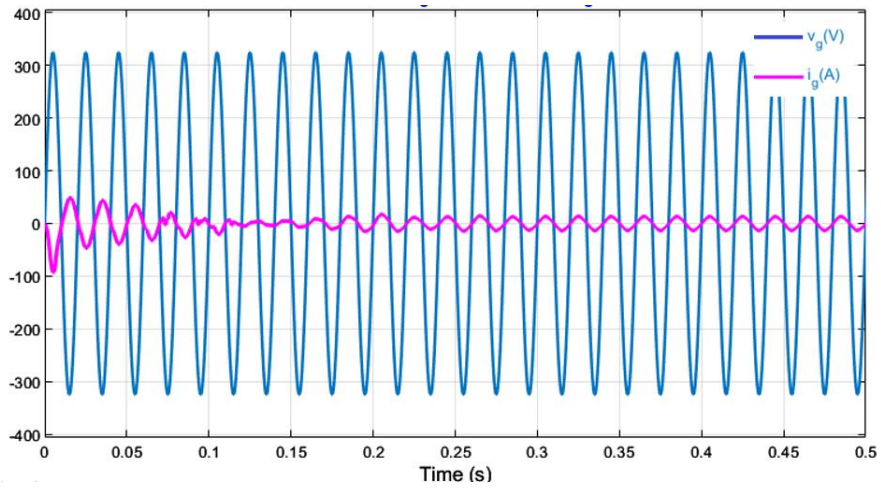

Figure 10. Voltage and current in the grid

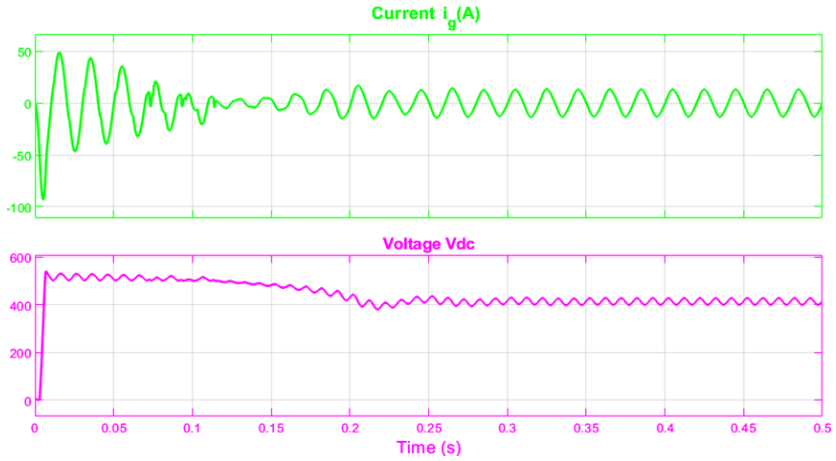

Figure 11. Current grid and DC link voltage

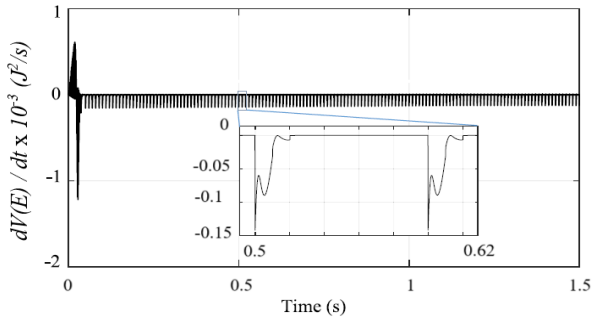

Figure 12. Derivative of the Lyapunov function $dV(E)/dt$

The performance of the control strategy adopted, whether based on MPPT with PI and the resonant proportional controller (PR), is validated by the system's response to a variable irradiance profile between 300 W/m² and 1000 W/m², under a constant temperature of 25 °C. This is illustrated in Figures 13 and 14, where the current intensity in the network, $I_g(t)$, varies and follows the evolution of the irradiation profile, with appropriate response time and dynamics. In addition, this V_{dc} voltage curve has a response time of approximately 0.2 s and an overshoot of 25%.

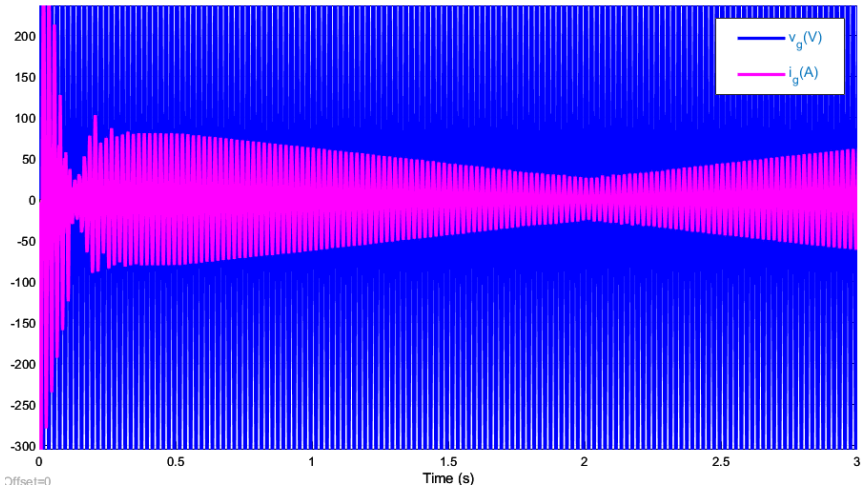

Figure 13. Voltage and current grid for a variable irradiation profile

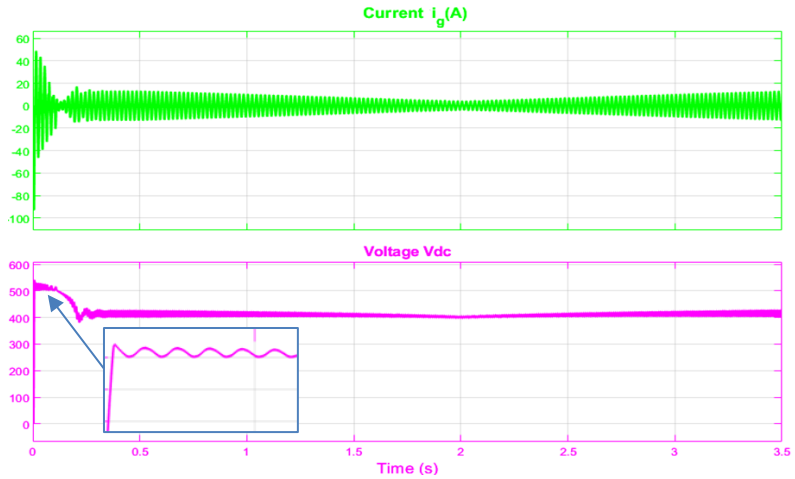

Figure 14. V_{dc} voltage of the connection DC-link and I_g current Grid for a variable irradiation profile

6. CONCLUSION

This study investigated a grid-connected single-phase photovoltaic system equipped with a DC/AC inverter, an MPPT algorithm, a PI controller for DC bus voltage regulation, and a PR controller for grid current injection. The MPPT ensures maximum power extraction from the PV array, while the PI controller maintains stable DC bus voltage under varying irradiance and load conditions. The PR controller allows accurate sinusoidal current injection into the grid, minimizing steady-state error and improving disturbance rejection compared to a conventional PI controller. Simulation results confirm that the combined use of the inverter and these control strategies guarantee overall system stability and efficient, reliable operation of the grid-connected PV system.

Stability is typically limited to the right side of the PV curve (V_{pv}>V_{MP}) without a voltage controller, while the left side (V_{pv}<V_{MP}) remains unstable. Introducing a PI controller to regulate energy via the DC-link capacitor ensures system stability across all operating points. Using a Lyapunov function based on the DC bus capacitor's energy, the derivative reveals the dynamics of stored energy and ensures stability. A theoretical analysis was performed to optimize the performance of a grid-connected single-phase DC/AC inverter.

Simulations were carried out and validated in MATLAB/Simulink for a 2 kW system, demonstrating satisfactory performance. The results indicate that a PR regulator can overcome the limitations of the PI regulator, including its inability to track a sinusoidal reference without steady-state error and its limited disturbance rejection. Stability analysis shows that instability originates from the inverse error signal at the input of the DC voltage regulator.

This research facilitates the integration of large-scale PV systems into smart grids, thus contributing to the energy transition. The simulated system can be integrated into smart grids, enabling dynamic management of load, storage and forecasting of PV production. It also offers potential for use in urban, rural or isolated areas, thanks to improved grid compatibility and optimized energy management. In particular, it offers an opportunity to implement such a grid-connected photovoltaic system using a Semikron-type experimental bench materializing the inverter, with simulated controllers implemented using a dSPACE 1104 board combined with MATLAB/Simulink. This research will provide a solid basis for the realization of single-stage three-phase photovoltaic systems associated with a grid-connected three-phase inverter.

FUNDING INFORMATION

Authors state no funding involved.

CONFLICT OF INTEREST STATEMENT

Authors state no conflict of interest.

DATA AVAILABILITY

Data availability is not applicable to this paper as no new data were created or analyzed in this study.

REFERENCES

[1] R. K. Jones and S. Kurtz, "Optimizing the configuration of photovoltaic plants to minimize the need for storage," *IEEE Journal of Photovoltaics*, vol. 12, no. 3, pp. 860–870, May 2022, doi: 10.1109/JPHOTOV.2022.3157565.

[2] A. Kabba, H. El Fadil, A. M. Hamed, A. Yahya, and F. Giri, "A high gain observer design for the three-phase shunt active power filter interfacing a photovoltaic source," *IFAC-PapersOnLine*, vol. 55, no. 12, pp. 306–311, Jan. 2022, doi: 10.1016/j.ifacol.2022.07.329.

[3] E. Radwan, K. Salih, E. Awada, and M. Nour, "Modified phase locked loop for grid connected single phase inverter," *International Journal of Electrical and Computer Engineering*, vol. 9, no. 5, pp. 3934–3943, Oct. 2019, doi: 10.11591/ijece.v9i5.pp3934-3943.

[4] A. Ahmad, H. D. Tafti, G. Konstantinou, B. Hredzak, and J. E. Fletcher, "Distributed photovoltaic inverters' response to voltage phase-angle jump," *IEEE Journal of Photovoltaics*, vol. 12, no. 1, pp. 429–436, Jan. 2022, doi: 10.1109/JPHOTOV.2021.3128818.

[5] M. U. Hassan, M. I. Nawaz, and J. Iqbal, "Towards autonomous cleaning of photovoltaic modules: Design and realization of a robotic cleaner," in *2017 1st International Conference on Latest Trends in Electrical Engineering and Computing Technologies, INTELLECT 2017*, Nov. 2017, vol. 2018-January, pp. 1–6, doi: 10.1109/INTELLECT.2017.8277631.

[6] E. Radwan, M. Nour, A. Baniyounes, and K. S. Al-Olimat, "Design of type-1 servo controller for grid voltage modulated direct-power control of single-phase grid-connected PV inverter," *International Journal of Electrical and Computer Engineering*, vol. 11, no. 3, pp. 1912–1923, Jun. 2021, doi: 10.11591/ijece.v11i3.pp1912-1923.

[7] O. Ceylan, S. Paudyal, and I. Pisica, "Nodal sensitivity-based smart inverter control for voltage regulation in distribution feeder," *IEEE Journal of Photovoltaics*, vol. 11, no. 4, pp. 1105–1113, Jul. 2021, doi: 10.1109/JPHOTOV.2021.3070416.

[8] H. Colin, C. Duvauchelle, G. Moine, Y. Tanguy, B. Gaiddon, and T. Tran-Quoc, "Pre-normative scientific studies on the connection to the grid of photovoltaic technical installations - ESPRIT. Connection of photovoltaic installations to the low voltage public power grid. Regulatory framework, impacts and recommendations," (in French), International Atomic Energy Agency (IAEA), France, Report no. INIS-FR--20-0158, 2010.

[9] T. Abderrahim, T. Abdelwahed, and M. Radouane, "Improved strategy of an MPPT based on the sliding mode control for a PV system," *International Journal of Electrical and Computer Engineering*, vol. 10, no. 3, pp. 3074–3085, Jun. 2020, doi: 10.11591/ijece.v10i3.pp3074-3085.

[10] M. N. H. Khan, M. Forouzesh, Y. P. Siwakoti, L. Li, T. Kerekes, and F. Blaabjerg, "Transformerless inverter topologies for single-phase photovoltaic systems: a comparative review," *IEEE Journal of Emerging and Selected Topics in Power Electronics*, vol. 8, no. 1, pp. 805–835, Mar. 2020, doi: 10.1109/JESTPE.2019.2908672.

[11] R. Au *et al.*, "Advanced non-linear control of a grid-connected photovoltaic system," (in French), in *CMSI FES*, 2016.

[12] C. Aouadi, A. Abouloifa, A. Hamdoun, and Y. Boussairi, "Advanced nonlinear control of photovoltaic system connected to the grid," in *2014 2nd World Conference on Complex Systems, WCCS 2014*, Nov. 2014, pp. 61–66, doi: 10.1109/ICoCS.2014.7060954.

[13] M. Barghi Latran and A. Teke, "Investigation of multilevel multifunctional grid connected inverter topologies and control strategies used in photovoltaic systems," *Renewable and Sustainable Energy Reviews*, vol. 42, pp. 361–376, Feb. 2015, doi: 10.1016/j.rser.2014.10.030.

[14] C. Aouadi, A. Abouloifa, A. Hamdoun, and Y. Boussairi, "Nonlinear controller design for single-phase grid-connected photovoltaic systems," in *Proceedings of 2015 IEEE International Renewable and Sustainable Energy Conference, IRSEC 2015*, Dec. 2016, pp. 1–5, doi: 10.1109/IRSEC.2015.7454953.

[15] A. S. Saleh, R. K. Antar, and A. J. Ali, "Design and implementation of single-phase PV power system," *Design Engineering*, vol. 25, no. 6, pp. 2147–2157, Sep. 2021.

[16] S. Golestan, J. M. Guerrero, and J. C. Vasquez, "Single-phase PLLs: A review of recent advances," *IEEE Transactions on Power Electronics*, vol. 32, no. 12, pp. 9013–9030, Dec. 2017, doi: 10.1109/TPEL.2017.2653861.

[17] D. G. Holmes and D. A. Martin, "Implementation of a direct digital predictive current controller for single and three phase voltage source inverters," in *Conference Record - IAS Annual Meeting (IEEE Industry Applications Society)*, 1996, vol. 2, pp. 906–913, doi: 10.1109/ias.1996.560191.

[18] A. Tilli and A. Tonielli, "Sequential design of hysteresis current controller for three-phase inverter," *IEEE Transactions on Industrial Electronics*, vol. 45, no. 5, pp. 771–781, Oct. 1998, doi: 10.1109/41.720334.

[19] M. Brahmi, C. B. Regaya, H. Hamdi, and A. Zaafouri, "Comparative study of P&O and PSO MPPT controllers for photovoltaic systems," in *2022 8th International Conference on Control, Decision and Information Technologies (CoDIT)*, May 2022, pp. 1608–1613, doi: 10.1109/CoDIT55151.2022.9804021.

[20] O. Saleem, S. Ali, and J. Iqbal, "Robust MPPT control of stand-alone photovoltaic systems via adaptive self-adjusting fractional order PID controller," *Energies*, vol. 16, no. 13, 2023, doi: 10.3390/en16135039.

[21] I. U. Haq *et al.*, "Neural network-based adaptive global sliding mode MPPT controller design for stand-alone photovoltaic systems," *PLoS ONE*, vol. 17, no. 1 January, p. e0260480, 2022, doi: 10.1371/journal.pone.0260480.

[22] N. A. Ashtiani, S. M. Azizi, and S. A. Khajehoddin, "Robust control design for high-power density PV converters in weak grids," *IEEE Transactions on Control Systems Technology*, vol. 27, no. 6, pp. 2361–2373, Nov. 2019, doi: 10.1109/TCST.2018.2867212.

[23] R. Errouissi, A. Al-Durra, and S. M. Muyeen, "Design and implementation of a nonlinear pi predictive controller for a grid-tied photovoltaic inverter," *IEEE Transactions on Industrial Electronics*, vol. 64, no. 2, pp. 1241–1250, Feb. 2017, doi: 10.1109/TIE.2016.2618339.

[24] Y. Gui, F. Blaabjerg, X. Wang, J. D. Bendtsen, D. Yang, and J. Stoustrup, "Improved DC-link voltage regulation strategy for grid-connected converters," *IEEE Transactions on Industrial Electronics*, vol. 68, no. 6, pp. 4977–4987, Jun. 2021, doi: 10.1109/TIE.2020.2989720.

[25] F. El Aamri *et al.*, "Stability analysis for DC-link voltage controller design in single-stage single-phase grid-connected PV inverters," *IEEE Journal of Photovoltaics*, vol. 13, no. 4, pp. 580–589, Jul. 2023, doi: 10.1109/JPHOTOV.2023.3263253.

[26] F. El Aamri, H. Maker, D. Sera, S. V. Spataru, J. M. Guerrero, and A. Mouhsen, "A direct maximum power point tracking method for single-phase grid-connected PV inverters," *IEEE Transactions on Power Electronics*, vol. 33, no. 10, pp. 8961–8971, Oct. 2018, doi: 10.1109/TPEL.2017.2780858.

[27] K. Ma, W. Chen, M. Liserre, and F. Blaabjerg, "Power controllability of a three-phase converter with an unbalanced AC source," *IEEE Transactions on Power Electronics*, vol. 30, no. 3, pp. 1591–1604, Mar. 2015, doi: 10.1109/TPEL.2014.2314416.

[28] M. Rajeev and V. Agarwal, "Analysis and control of a novel transformer-less microinverter for PV-grid interface," *IEEE Journal of Photovoltaics*, vol. 8, no. 4, pp. 1110–1118, Jul. 2018, doi: 10.1109/JPHOTOV.2018.2825298.

[29] H. Komurcugil, N. Altin, S. Ozdemir, and I. Sefa, "An extended Lyapunov-function-based control strategy for single-phase UPS inverters," *IEEE Transactions on Power Electronics*, vol. 30, no. 7, pp. 3976–3983, 2015, doi: 10.1109/TPEL.2014.2347396.

BIOGRAPHIES OF AUTHORS

Abdelaziz Kabba received the B.S. degree in electronics and the aggregation degree in electrical engineering from ENSET, Mohammed V University, Rabat, Morocco, in 1994 and 2004, respectively. He obtained a diploma as a secondary school inspector in engineering sciences from the CNI in Rabat and a master's degree in electrical engineering from ENSAM, Mohammed V University, Rabat, Morocco, in 2020. He is currently a pedagogical inspector at the regional academy of education and training in Beni-Mellal, Morocco, and he is preparing his doctorate at ENSA, University Ibn Tofail, Kenitra, Morocco. His research interests include nonlinear control, power converters and renewable energies, smart microgrids and electric vehicles. Abdelaziz KABBA has participated in 6 international conferences and contributed to the publication of conference papers. He is a member of the Scientific Association for Automatic Control and Renewable Energies. He can be contacted by Mobile: +212 664 80 09 84 or e-mail: kabbaziz.70@gmail.com.

Abdellah Lassioui received his Diploma of State Engineer in electrical engineering from The University of Sciences and Techniques, Tangier, Morocco in 2015. He received his PhD in automatic control in 2021, University Ibn Tofail, Kenitra, Morocco. He is currently with the ISA Laboratory. Since 2022, he has been, successively Assistant Professor at the National School of Applied Sciences, University Ibn Tofail, Kenitra, Morocco. His current research interests include the fields of nonlinear control of power electronic systems, electric vehicles, and wireless power transfer charging for electric vehicles. He has co-authored over 40 journal and conference papers. He can be contacted by email: Abdellah.lassioui@uit.ac.ma.

Hassan El Fadil received the B.S. degree in electronics and the aggregation degree in electrical engineering from ENSET, Mohammed V University, Rabat, Morocco, in 1994 and 1999, respectively. He earned the M.S. and Ph.D. degrees in automatic control from EMI, Mohammed V University, Rabat, Morocco, in 2003 and 2008, respectively. He is currently a Professor at ENSA, Ibn Tofail University, Kenitra, Morocco, and serves as the Director of the ASE Laboratory. His research interests include nonlinear and adaptive control, power converters and electric motor control, renewable energy, distributed energy resources, smart grids, and electric vehicles. He has contributed to the edition of over 15 special issues and conference proceedings and has participated in more than 60 international conferences, including ten that he co-organized. He is a member of several international scientific societies and associations in the fields of automatic control and renewable energy. He has published over 160 journal and conference papers in his areas of expertise. Hassan El Fadil is with ISA Lab., ENSA, Ibn Tofail University, PO Box 242, 14000, Kenitra, Morocco. He can be contacted by Tel: +212 537 32 94 48; Mobile: +212 694 500 569; Fax: +212 537 32 92 47, email: elfadilhassan@yahoo.fr, hassan.elfadil@uit.ac.ma.